JOURNAL OF COMPUTATIONAL PHYSICS 7, 301–309 (1971)

A Comparison of First- and Second-Order Difference Approximations over a Spherical Geodesic Grid

DAVID L. WILLIAMSON

*National Center for Atmospheric Research,**
Boulder, Colorado 80302

Received August 21, 1970

Second-order difference approximations are derived for a primitive barotropic model over a spherical geodesic grid and are compared to first-order conservative approximations. The second-order approximation requires a viscosity term for stability. A given value of the viscosity coefficient reduces the high wavenumber noise more with the second-order scheme than with the first-order scheme.

1. INTRODUCTION

The recent use of a spherical domain for numerical atmospheric models has led to interest in improving finite-difference approximations for fluid flow on a sphere. Current spherical atmospheric models use approximations over grids defined by intersections of latitude and longitude circles. See, for example, Washington and Kasahara [1]. These grids must be modified near the poles for use with explicit approximations because the convergence of meridians, and hence grid points, approaching the poles imposes a very severe restriction on the maximum allowable time step through linear stability. The usual modification involves increasing the longitudinal grid increment ($\Delta\lambda$) in the neighborhood of the poles and suitably modifying the finite differences used in those regions. These schemes have reduced accuracy in the regions where the grid is modified [2].

In an attempt to avoid the problems associated with modifying a latitude-longitude grid, quasihomogeneous spherical grids were defined by Sadourny *et al* [3] and Williamson [4]. An example is shown in Fig. 1. These grids cover the sphere with almost equal-area, equilateral spherical triangles resulting in a variation in the grid interval of about 10% of the mean value. Preliminary tests in Refs. [3] and [4] showed these methods to be superior to the conventional approximations over

* The National Center for Atmospheric Research is sponsored by the National Science Foundation.

FIG. 1. Spherical geodesic grid used for computations reported in this paper.

latitude-longitude grids for the nondivergent barotropic vorticity equation. Comparison of methods for the primitive barotropic model is not as clear cut. Williamson [5] showed that the popular type of energy-conserving approximations [6] become first order when applied to the spherical geodesic grid because of the nonuniform nature of the grid intervals. The truncation error has a very adverse effect on the mass divergence computations with grids of resolution greater than $2\frac{1}{2}°$.

In this paper we derive second-order approximations over the spherical geodesic grid and compare results from these approximations with the results from the first-order conservative approximations.

2. APPROXIMATIONS

The equations to be integrated are those of the primitive barotropic model:

$$\begin{aligned} \frac{\partial h\mathbf{V}}{\partial t} + \nabla \cdot (\mathbf{V}h\mathbf{V}) + \mathbf{F} \times h\mathbf{V} + g\nabla \frac{h^2}{2} = 0, \\ \frac{\partial h}{\partial t} + \nabla \cdot (h\mathbf{V}) = 0, \end{aligned} \tag{1}$$

where h is the height of the free surface and $\mathbf{V}$ is the vector velocity with components u and v in spherical coordinates. $\mathbf{F}$ is $(f + (u/a) \tan \theta)\, \hat{k}$, where $\hat{k}$ is the radial outward unit vector, f is the Coriolis parameter, and a is the radius of the earth.

The conservative first-order approximations are given in [5] and are not repeated here. The second-order approximations discussed here are assumed to have the form of a linear combination of values at the center point and the first ring of surrounding points. The coefficients are chosen so that the Taylors' series expansion about the center point of the combination has a zero first-order error term.

The double Taylors' series in spherical polar coordinates is given by

$$\psi_i = \psi_0 + \sum_{j=1}^{\infty} \frac{1}{j!} \left[(\theta_i - \theta_0) \frac{\partial}{\partial \theta} + (\lambda_i - \lambda_0) \frac{\partial}{\partial \lambda} \right]^j \psi_0 , \tag{2}$$

where the subscript 0 denotes the point at which the approximation is applied and i denotes one of the surrounding points (see Fig. 2 or Ref. [7] for definition of local polar subscripting used here).

In the following we give an example of how the approximations are derived. Let D be an approximation to the divergence $\nabla \cdot \mathbf{V}$ and suppose D has the form

$$D = \sum_{i=1}^{k} \mathbf{c}_i \cdot (\mathbf{V}_i - \mathbf{V}_0) + \mathbf{c}_0 \cdot \mathbf{V}_0 , \tag{3}$$

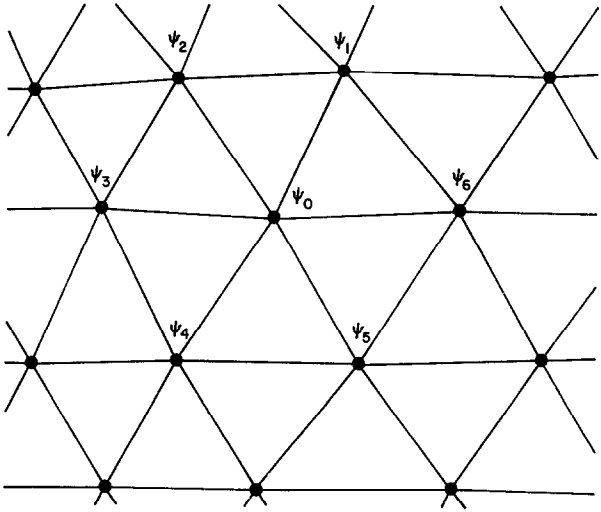

FIG. 2. Illustration of subscripts used in the finite-difference approximations.

where $\mathbf{c}_i$ are the coefficients to be determined so that D is second order. Substitution of (2) into (3) and rearranging yield

$$D = \mathbf{c}_0 \cdot \mathbf{V}_0 + \frac{\partial \mathbf{V}}{\partial \theta} \cdot \sum_{i=1}^{k} \mathbf{c}_i(\theta_i - \theta_0) + \frac{\partial \mathbf{V}}{\partial \lambda} \cdot \sum_{i=1}^{k} \mathbf{c}_i(\lambda_i - \lambda_0)$$

$$+ \frac{\partial^2 \mathbf{V}}{\partial \theta^2} \cdot \frac{1}{2} \sum_{i=1}^{k} \mathbf{c}_i(\theta_i - \theta_0)^2 + \frac{\partial^2 \mathbf{V}}{\partial \theta\, \partial \lambda} \cdot \sum_{i=1}^{k} \mathbf{c}_i(\theta_i - \theta_0)(\lambda_i - \lambda_0)$$

$$+ \frac{\partial^2 \mathbf{V}}{\partial \lambda^2} \cdot \frac{1}{2} \sum_{i=1}^{k} \mathbf{c}_i(\lambda_i - \lambda_0)^2 + O(\Delta^3).$$

Thus, requiring D be second order gives the following set of equations for the coefficients $\mathbf{c}_i$:

$$\mathbf{c}_0 = -\frac{\tan \theta}{a} \hat{j}; \tag{4}$$

$$\sum_{i=1}^{k} (\theta_i - \theta_0)\, \mathbf{c}_i = \frac{1}{a} \hat{j}, \tag{5a}$$

$$\sum_{i=1}^{k} (\lambda_i - \lambda_0)\, \mathbf{c}_i = \frac{1}{a \cos \theta} \hat{\imath}, \tag{5b}$$

$$\sum_{i=1}^{k} (\theta_i - \theta_0)^2\, \mathbf{c}_i = 0, \tag{5c}$$

$$\sum_{i=1}^{k} (\theta_i - \theta_0)(\lambda_i - \lambda_0)\, \mathbf{c}_i = 0, \tag{5d}$$

$$\sum_{i=1}^{k} (\lambda_i - \lambda_0)^2\, \mathbf{c}_i = 0, \tag{5e}$$

where $\hat{\imath}$ is the unit vector in the longitudinal direction and $\hat{j}$ is the unit vector in the latitudinal direction. Equations (5) are a set of five vector equations in k vector unknowns $\mathbf{c}_1, \mathbf{c}_2, \ldots, \mathbf{c}_k$.

Consider now an approximation $\mathbf{G}$ to the gradient ∇h of the form

$$\mathbf{G} = \sum_{i=1}^{k} \mathbf{d}_i(h_i - h_0) + \mathbf{d}_0 h_0 . \tag{6}$$

Substitution of the Taylors' series for h_i, requiring second-order accuracy, gives

$$\mathbf{d}_0 = 0$$

and

$$\mathbf{d}_i = \mathbf{c}_i, \qquad i = 1, 2, \ldots, k,$$

where $\mathbf{c}_i$ are the solution to Eqs. (5).

Similarly, the following second-order approximations are easily obtained:

$$\nabla h^2 \doteq \sum_{i=1}^{k} \mathbf{c}_i(h_i^2 - h_0^2), \tag{7}$$

$$\nabla \cdot (h\mathbf{V}) \doteq \sum_{i=1}^{k} \mathbf{c}_i \cdot (h_i\mathbf{V}_i - h_0\mathbf{V}_0) + \mathbf{c}_0 \cdot (h_0\mathbf{V}_0), \tag{8}$$

$$\nabla \cdot (\mathbf{V}h\mathbf{V}) \doteq \sum_{i=1}^{k} \mathbf{c}_i \cdot (\mathbf{V}_i h_i \mathbf{V}_i - \mathbf{V}_0 h_0 \mathbf{V}_0) + \mathbf{c}_0 \cdot (\mathbf{V}_0 h \mathbf{V}_0), \tag{9}$$

where the coefficients $\mathbf{c}_i$ are solutions to Eqs. (5).

In order to apply the approximations listed above, Eqs. (5) must be solved at each grid point. These are a set of five equations in k unknowns where k is the number of grid points surrounding the point at which the approximations are applicable. Twelve grid points of the spherical geodesic grid have five surrounding points. At these points Eqs. (5) are sufficient to solve for the five coefficients. The other grid points have six surrounding grid points and hence six unknowns. One more equation is needed for a unique solution.

A possible extra equation is formed by requiring that a higher-order error term such as $\partial^3/\partial\theta^3$ also be zero. However, no *one* condition was found for which the matrix was nonsingular at every grid point.

The coefficients used for the computations reported here were derived in the following way: One of the six surrounding grid points is neglected and the remaining five points are used to define an approximation involving only five of the surrounding grid points. The five coefficients are obtained by solving Eqs. (5). Next, a different surrounding point is neglected and an approximation is defined over a different set of five surrounding points. This process is repeated neglecting each of the surrounding points. Thus, six different approximations are defined, each involving a different set of five of the surrounding points. These six approximations, or sets of coefficients, are then averaged to obtain an approximation using all six surrounding points.

3. Results

Equations (1) were integrated using approximations (6)–(8) with Euler-backward [8] time stepping. The initial conditions given in Ref. [5] are for a wave which, in a nondivergent barotropic atmosphere, moves without change of shape. The analytic solution is not known for the divergent model. The second-order approximations were found to be unstable when no viscosity term was included in the equations. The stability did not improve by decreasing the time step indicating perhaps nonlinear instability. A viscous term of the form $\nu h\nabla^2\mathbf{V}$ was added to the momentum equation. With a suitable value of ν this term stabilized the scheme. The finite-difference form of the ∇^2 operator is given in Ref. [4].

Figure 3 shows height fields from six-day integrations using first-order scheme IIs of Ref. [5] for various resolutions and viscosity coefficients. Figure 4 shows height fields from the second-order scheme for the same cases. The time steps used were 20 min for first-order 5° grid, 10 min for first-order $2\frac{1}{2}$° grid, 10 min for second-order 5° grid, and 5 min for second-order $2\frac{1}{2}$° grid. When these time steps

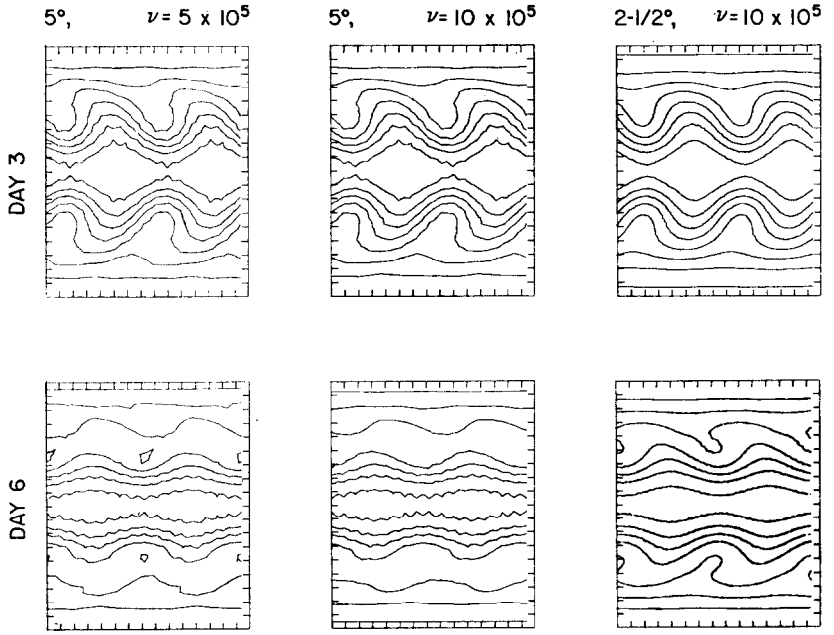

FIG. 3. Height fields produced by the first-order conservative scheme. The region covered by each figure is −90° to +90° latitude and 0° to 150° longitude, a little over two periods of the initial conditions.

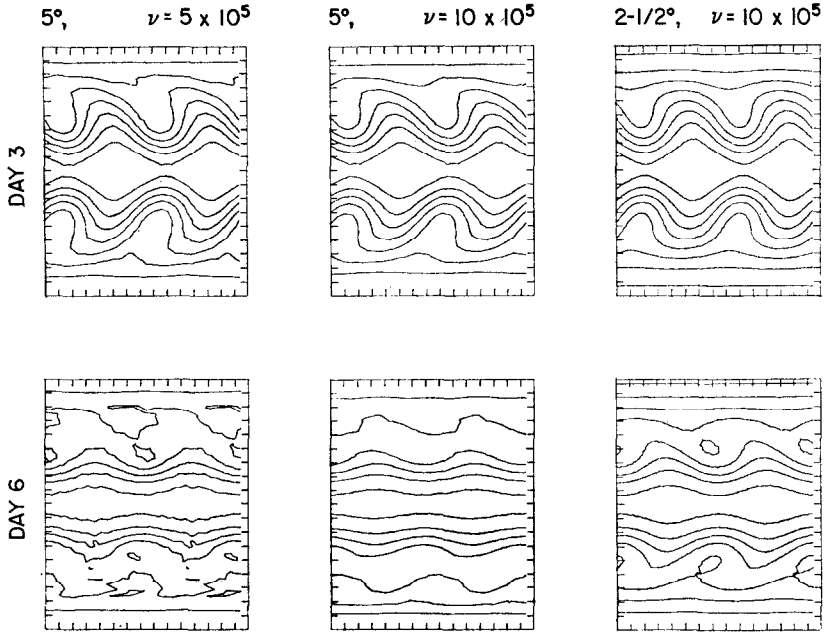

FIG. 4. Height fields produced by the second-order scheme. The region covered by each figure is the same as Fig. 3.

were doubled, the schemes were unstable. The linear stability condition is difficult to calculate for the spherical geodesic schemes. The condition would be slightly different at each grid point since the coefficients are different at each grid point. The integrations of the second-order scheme required twice as much computer time as the first-order scheme. This difference is mainly due to the difference of the maximum stable time steps of the two cases. The first column of both figures is for a 5° grid with ν equal to 5×10^5 m^2 sec^{-1}. The second column is for a 5° grid with ν equal to 10×10^5 m^2 sec^{-1}. The value of 5×10^5 is close to the value given by Richardson [9] for the 5° mesh size. As can be seen, it does not eliminate the small-scale noise. The second-order scheme has less small-scale noise than the first-order scheme. The value of 10×10^5 keeps the second-order scheme stable, but damps the main wave considerably.

Integrations with second-order schemes over the $2\frac{1}{2}°$ grid seem to be more unstable than over the 5° grid. Integrations with ν equal to 5×10^5 showed much higher amplitude in the two-grid interval wave with the second-order scheme over the $2\frac{1}{2}°$ grid than with the 5° grid at day 6. Results with $\nu = 10 \times 10^5$ over the $2\frac{1}{2}°$ grid are shown in the right column of the figures. The wave is seen to have a larger amplitude than the 5° case with the same value of ν. Again, the second-order scheme has less small-scale noise than the first-order scheme.

TABLE I

Order	Resolution	$\nu \times 10^5$ m^2 sec^{-1}	Energy $\times 10^8$ m^3 sec^{-2}	
			Day 3	Day 6
1	5°	5	4.579	4.564
1	5°	10	4.569	4.553
1	2½°	10	4.576	4.556
2	5°	5	4.587	4.583
2	5°	10	4.576	4.556
2	2½°	10	4.581	4.569

The total energy for the above cases is listed in Table I for day 3 and day 6. The initial energy was 4.616×10^8 m^3 sec^{-2}. Both kinetic and potential energies decreased monotonically during the six days. In all of the cases the energy decreased more during the first three days than during the last three. This is probably caused by an initial adjustment of the velocity and height fields. It is seen again that the 2½° cases have less total damping than the 5° cases with the same value of ν and the second-order scheme has slightly less damping than the first-order scheme.

4. Conclusions

These second-order approximations eliminate the errors observed in an earlier paper in mass flux calculations using first-order conservative schemes over 5° grids. The second-order schemes, however, require a relatively large viscosity coefficient to prevent instability. With viscosity included the solution produced by the second-order scheme has less high wavenumber noise than the solution produced by the first-order scheme using the same value of the viscosity coefficient. The large-scale patterns of the two solutions are very similar.

Acknowledgment

The author would like to thank Dr. Akira Kasahara for many helpful comments on the original manuscript.

References

1. W. Washington and A. Kasahara, A January simulation experiment with the two-layer version of the NCAR global circulation model, *Mon. Wea. Rev.* **98** (1970), 559–580.
2. J. M. Gary, A comparison of difference schemes used for numerical weather prediction, *J. Comp. Phys.* **4** (1969), 279–305.

3. R. SADOURNY, A. ARAKAWA, AND Y. MINTZ, Integration of the nondivergent barotropic vorticity equation with an icosahedral-hexagonal grid for the sphere, *Mon. Wea. Rev.* **96** (1968), 351–356.
4. D. WILLIAMSON, Integration of the barotropic vorticity equation on a spherical geodesic grid, *Tellus* **20** (1968), 642–653.
5. D. WILLIAMSON, Integration of the primitive barotropic model over a spherical geodesic grid, *Mon. Wea. Rev.* **98** (1970), 512–520.
6. K. BRYAN, A scheme for numerical integration of the equations of motion on an irregular grid free of nonlinear instability, *Mon. Wea. Rev.* **94** (1966), 39–40.
7. D. WILLIAMSON, Numerical integration of fluid flow over triangular grids, *Mon. Wea. Rev.* **97** (1969), 885–895.
8. Y. KURIHARA, On the use of implicit and iterative methods for the time integration of the wave equation, *Mon. Wea. Rev.* **93** (1965), 33–46.
9. L. F. RICHARDSON, Atmospheric diffusion shown on a distance neighbour graph, *Proc. Roy. Soc. Ser. A* **110** (1926), 709–737.